

Probing model-independent limits on $W^+W^-\gamma$ triple gauge boson vertex at the LHeC and the FCC-he

A. Gutiérrez-Rodríguez^{*,1} M. Köksal^{†,2} A. A. Billur^{‡,3} and M. A. Hernández-Ruíz^{§4}

¹*Facultad de Física, Universidad Autónoma de Zacatecas*

Apartado Postal C-580, 98060 Zacatecas, México.

²*Department of Optical Engineering, Sivas Cumhuriyet University, 58140, Sivas, Turkey.*

³*Department of Physics, Sivas Cumhuriyet University, 58140, Sivas, Turkey.*

⁴*Unidad Académica de Ciencias Químicas, Universidad Autónoma de Zacatecas*

Apartado Postal C-585, 98060 Zacatecas, México.

(Dated: October 8, 2019)

Abstract

We study the cross-section of production of a single W^- boson in association with a neutrino through the process $e^-p \rightarrow e^-\gamma^*p \rightarrow \nu_e W^-p$. Additionally, we obtain the anomalous couplings $\Delta\kappa_\gamma$ and λ_γ of the $W^+W^-\gamma$ vertex at the Large Hadron Electron Collider (LHeC) and the Future Circular Collider Hadron-Electron (FCC-he). The impact of the polarized beam due to the electron is also analyzed. Our best limits for $\Delta\kappa_\gamma$ and λ_γ at the 95% C.L. are: $\Delta\kappa_\gamma = \pm 0.0017$, $\lambda_\gamma = \pm 0.0053$ (unpolarized electron beam) and $\Delta\kappa_\gamma = \pm 0.0013$, $\lambda_\gamma = \pm 0.0046$ (polarized electron beam) identifying the W^- boson through the hadronic decay channel. In addition, the $e^-\gamma^* \rightarrow \nu_e W^-$ collision is one of the clean, pure and simple process to probe the $W^+W^-\gamma$ coupling without the complications of QCD backgrounds.

PACS numbers: 12.60.-i, 14.70.Fm, 4.70.Bh

Keywords: Models beyond the standard model, W bosons, Triple gauge boson couplings.

* alexgu@fisica.uaz.edu.mx

† mkoksal@cumhuriyet.edu.tr

‡ abillur@cumhuriyet.edu.tr

§ mahernan@uaz.edu.mx

I. INTRODUCTION

The Standard Model (SM) of elementary particle physics based on the gauge group $SU(2)_L \times U(1)_Y$, describes the electroweak interactions as being mediated by the γ -photon, the Z -boson and the W^\pm -bosons [1–3].

The W^\pm -bosons are among the heaviest particles known of the SM. Although the properties of the W^\pm -bosons have been studied for many years, measuring its mass, as well as its anomalous couplings with high precision remains a great challenge and an important objective to prove the unification of the electromagnetic and weak interactions in the SM. High precision measurement of the properties of these bosons has made these particles one of the most attractive particles for new physics research.

It is worth mentioning that it is very important to measure the masses of the W^\pm -bosons, as well as its anomalous couplings, as accurately as possible to better understand the Higgs boson, refine the SM and test its global consistency.

The $\nu_e W^-$ production at the e^-p colliders contains a lot of information on the existence of trilinear self-couplings among $W^+W^-\gamma$ gauge bosons. These couplings in a consequence of the non-Abelian gauge structure of the SM, predict the existence of the triple couplings $W^+W^-\gamma$ [1–3]. The $W^+W^-\gamma$ triple gauge boson vertex is accessible at the present and future colliders such as the Large Hadron Collider (LHC), the Large Hadron Electron Collider (LHeC), the Future Circular Collider Hadron-Electron (FCC-he) and the Compact Linear Collider (CLIC) at CERN for the post LHC era.

Under these arguments, in this paper, we study and present our results on the cross-section of the process $e^-p \rightarrow e^- \gamma^* p \rightarrow \nu_e W^- p$. In addition, we obtain model-independent limits on the anomalous electromagnetic couplings $\Delta\kappa_\gamma$ and λ_γ of the $W^+W^-\gamma$ vertex for the high-energies of the center-of mass energies $\sqrt{s} = 1.30, 1.98, 7.07, 10$ TeV and high-luminosities $\mathcal{L} = 10 - 1000 \text{ fb}^{-1}$ of the LHeC and the FCC-he [4–9]. We consider unpolarized and polarized electron beam.

A summary of experimental and phenomenological limits at 95% C.L. on the anomalous triple gauge boson couplings $\Delta\kappa_\gamma$ and λ_γ from the present and future colliders are given in Table I of Ref. [10]. See Refs. [11–25] for other limits on the anomalous $W^+W^-\gamma$ coupling in different contexts.

This work is organized as follows: In Sect. II we give an overview of the operators in our

effective Lagrangian. In Sect. III we derive limits on the anomalous couplings $\Delta\kappa_\gamma$ and λ_γ at the LHeC and the FCC-he. In Sect. IV we present our conclusions.

II. THE TRIPLE GAUGE BOSON VERTEX $W^+W^-\gamma$ WITH ANOMALOUS CONTRIBUTION

An appropriate model-independent context for describing possible new physics effects is based on effective Lagrangian. In this context, all the heavy degrees of freedom are integrated out to obtain effective interactions between the SM particles. This is justified since the related observables have so far not shown any significant deviation from the SM predictions.

We start from the effective Lagrangian formalism to study the process $e^-p \rightarrow e^-\gamma^*p \rightarrow \nu_e W^- p$, as well as to determine limits on the anomalous couplings $\Delta\kappa_\gamma$ and λ_γ . In this regard, our starting point is the effective Lagrangian \mathcal{L}_{eff} for the $W^+W^-\gamma$ interaction of the photon and the gauge bosons with operators up to mass dimension-six. Then \mathcal{L}_{eff} can be expanded as:

$$\mathcal{L}_{eff} = \mathcal{L}_{SM}^{(4)} + \sum_i \frac{C_i^{(6)}}{\Lambda^2} \mathcal{O}_i^{(6)} + \text{h.c.}, \quad (1)$$

where $\mathcal{L}_{SM}^{(4)}$ denotes the renormalizable SM Lagrangian and the non-SM part contains $\mathcal{O}_i^{(6)}$ the gauge-invariant operators of mass dimension-six. The index i runs over all operators of the given mass dimension. The mass scale is set by Λ , and the coefficients C_i are dimensionless parameters, which are determined once the full theory is known.

Thus effective Lagrangian relevant to our analysis of $\Delta\kappa_\gamma$ and λ_γ is given by:

$$\mathcal{L}_{eff} = \frac{1}{\Lambda^2} \left[C_W \mathcal{O}_W + C_B \mathcal{O}_B + C_{WWW} \mathcal{O}_{WWW} + \text{h.c.} \right], \quad (2)$$

with

$$\mathcal{O}_W = (D_\mu \Phi)^\dagger \hat{W}^{\mu\nu} (D_\nu \Phi), \quad (3)$$

$$\mathcal{O}_B = (D_\mu \Phi)^\dagger \hat{B}^{\mu\nu} (D_\nu \Phi), \quad (4)$$

$$\mathcal{O}_{WWW} = \text{Tr} [\hat{W}^{\mu\nu} \hat{W}_\nu^\rho \hat{W}_{\mu\rho}], \quad (5)$$

where D_μ is the covariant derivative, Φ is the Higgs doublet field and $\hat{B}_{\mu\nu}$, and $\hat{W}_{\mu\nu}$ are the $U(1)_Y$ and $SU(2)_L$ gauge field strength tensors. The coefficients of these operators C_W/Λ^2 , C_B/Λ^2 , and C_{WW}/Λ^2 , are zero in the SM.

With this methodology, the effective Lagrangian for describing the $W^+W^-\gamma$ coupling can be parameterized as [12, 26]:

$$\mathcal{L}_{WW\gamma} = -ig_{WW\gamma} \left[g_1^\gamma (W_{\mu\nu}^\dagger W^\mu A^\nu - W^{\mu\nu} W_\mu^\dagger A_\nu) + \kappa_\gamma W_\mu^\dagger W_\nu A^{\mu\nu} + \frac{\lambda_\gamma}{M_W^2} W_{\rho\mu}^\dagger W_\nu^\mu A^{\nu\rho} \right], \quad (6)$$

where $g_{WW\gamma} = e$, $V_{\mu\nu} = \partial_\mu V_\nu - \partial_\nu V_\mu$ with $V_\mu = W_\mu, A_\mu$. The couplings g_1^γ , κ_γ and λ_γ CP-preserving, and in the SM, $g_1^\gamma = \kappa_\gamma = 1$ and $\lambda_\gamma = 0$ at the tree level.

From Eq. (2), the operators of dimension-six are related to the anomalous triple gauge boson couplings as [13, 27, 28]:

$$\kappa_\gamma = 1 + \Delta\kappa_\gamma, \quad (7)$$

with

$$\Delta\kappa_\gamma = C_W + C_B, \quad (8)$$

$$\lambda_\gamma = C_{WW}. \quad (9)$$

From the effective Lagrangian given in Eq. (6), the Feynman rule for the anomalous $W^+W^-\gamma$ vertex function the most general CP-conserving and that is consistent with gauge and Lorentz invariance of the SM is given by [12]:

$$\begin{aligned} \Gamma_{\mu\nu\rho}^{WW\gamma} = & e \left[g_{\mu\nu}(p_1 - p_2)_\rho + g_{\nu\rho}(p_2 - p_3)_\mu + g_{\rho\mu}(p_3 - p_1)_\nu + \Delta\kappa_\gamma (g_{\rho\mu}p_{3\nu} - g_{\nu\rho}p_{3\mu}) \right. \\ & + \frac{\lambda_\gamma}{M_W^2} (p_{1\rho}p_{2\mu}p_{3\nu} - p_{1\nu}p_{2\rho}p_{3\mu} - g_{\mu\nu}(p_2 \cdot p_3 p_{1\rho} - p_3 \cdot p_1 p_{2\rho}) \\ & \left. - g_{\nu\rho}(p_3 \cdot p_1 p_{2\mu} - p_1 \cdot p_2 p_{3\mu}) - g_{\mu\rho}(p_1 \cdot p_2 p_{3\nu} - p_2 \cdot p_3 p_{1\nu}) \right], \quad (10) \end{aligned}$$

where the first three terms in Eq. (10) corresponds to the SM couplings, while the terms with $\Delta\kappa_\gamma$ and λ_γ give rise to the anomalous triple gauge boson couplings.

Different searches on these anomalous $W^+W^-\gamma$ couplings $\Delta\kappa_\gamma$ and λ_γ were performed by the LEP, the Tevatron and the LHC experiments, as shown in Table I of Ref. [10].

III. CROSS-SECTION OF THE PROCESS $e^-p \rightarrow e^-\gamma^*p \rightarrow \nu_e W^-p$ AND LIMITS ON THE ANOMALOUS COUPLINGS $\Delta\kappa_\gamma$ AND λ_γ

A. Cross-section of the process $e^-p \rightarrow e^-\gamma^*p \rightarrow \nu_e W^-p$ at the LHeC and the FCC-he

The LHeC and the FCC-he are proposed, designed and planned colliders to carry out e^-p collisions at center-of-mass energies $\sqrt{s} = 1.30, 1.97, 7.07$ and 10 TeV, that is to say with a four main stage research region [4–9]. The e^-p colliders can also be operated as $e^-\gamma^*$, γ^*p and $\gamma^*\gamma$ collider. This enables the investigation of the $e\gamma^*$ interactions where the emitted quasi-real photon γ^* is scattered with small angles from the beam pipe of e^- [29–34]. Since these photons have a low virtuality, they are almost on the mass shell. These processes can be described by the Equivalent Photon Approximation (EPA) [32, 35, 36], using the Weizsacker-Williams Approximation (WWA). The EPA has a lot of advantages such as providing the skill to reach crude numerical predictions via simple formulae. Furthermore, it may principally ease the experimental analysis because it enables one to directly achieve a rough cross-section for $e^-\gamma^* \rightarrow X$ process via the examination of the main process $e^-p \rightarrow e^-Xp$ where X represents objects produced in the final state. The production of high mass objects is particularly interesting at the e^-p colliders and the production rate of massive objects is limited by the photon luminosity at high invariant mass while the $e\gamma^*$ process at the e^-p colliders arises from quasi-real photon emitted from the incoming beams. In many studies, new physics investigations are examined by using the EPA [37–57].

Another very important element in our study corresponds to the impact of the polarization of the electron beam. About this, in the baseline LHeC and FCC-he design, the electron beam can be polarized up to $\pm 80\%$. By selecting different beam polarizations it is possible to enhance or suppress different physical processes. In the particular case of the process $e^-p \rightarrow e^-\gamma^*p \rightarrow \nu_e W^-p$, the chiral nature of the weak coupling to fermions can result in significant possible enhancements in $\nu_e W^-$ production. Starting from this, the polarized e^- beam combined with the clean experimental environment provided by the LHeC and the FCC-he will allow to improve strongly the potential of searches for the $W^+W^-\gamma$ triple gauge boson vertex. With these arguments, we consider polarized electron beam in our study. The expression for the total cross-section for an arbitrary degree of longitudinal e^- beam polarization is given by [58]:

$$\sigma_{e_r^-} = \sigma_{e_0^-} \cdot (1 - P_{e_r^-}), \quad \sigma_{e_l^-} + \sigma_{e_r^-} = 2\sigma_{e_0^-}, \quad (11)$$

where $\sigma_{e_r^-}$, $\sigma_{e_l^-}$ and $\sigma_{e_0^-}$ represent the right, left and without electron beam polarization, respectively and P_{e^-} is the polarization degree of the electron.

The schematic diagram corresponding to the process $e^-p \rightarrow e^- \gamma^* p \rightarrow \nu_e W^- p$ is given in Fig. 1. While the representative leading order Feynman diagrams for the subprocess $\gamma^* e^- \rightarrow \nu_e W^-$ are depicted in Fig. 2. We based our calculations on electron-photon fluxes through the subprocess $e^- \gamma^* \rightarrow \nu_e W^-$. In addition, it is evident the contribution of elastic process with an intact proton in the final state.

Finally, the total cross-section is obtained by folding the elementary cross-section with the photon distribution function:

$$\sigma(e^-p \rightarrow e^- \gamma^* p \rightarrow \nu_e W^- p) = \int f_{\gamma^*}(x) \hat{\sigma}(e^- \gamma^* \rightarrow \nu_e W^-) dx, \quad (12)$$

where $\hat{\sigma}(e^- \gamma^* \rightarrow \nu_e W^-)$ is the cross-section for the reaction $e^- \gamma^* \rightarrow \nu_e W^-$, and the distribution function $f_{\gamma^*}(x)$ of the EPA photons which are emitted by proton is given by [32, 59]:

$$f_{\gamma^*}(x) = \frac{\alpha}{\pi E_p} \left\{ [1-x] \left[\varphi\left(\frac{Q_{max}^2}{Q_0^2}\right) - \varphi\left(\frac{Q_{min}^2}{Q_0^2}\right) \right] \right\}, \quad (13)$$

where $x = E_\gamma/E_p$ and Q_{max}^2 is the maximum virtuality of the photon. For our calculations, we use $Q_{max}^2 = 2 \text{ GeV}^2$. The minimum value of the Q_{min}^2 is:

$$Q_{min}^2 = \frac{m_p^2 x^2}{1-x}. \quad (14)$$

From Eq. (13), the function φ is given by:

$$\begin{aligned} \varphi(\theta) = & (1+ay) \left[-\ln\left(1+\frac{1}{\theta}\right) + \sum_{k=1}^3 \frac{1}{k(1+\theta)^k} \right] + \frac{y(1-b)}{4\theta(1+\theta)^3} \\ & + c\left(1+\frac{y}{4}\right) \left[\ln\left(\frac{1-b+\theta}{1+\theta}\right) + \sum_{k=1}^3 \frac{b^k}{k(1+\theta)^k} \right], \end{aligned} \quad (15)$$

where explicitly y , a , b and c are as follows:

$$y = \frac{x^2}{(1-x)}, \quad (16)$$

$$a = \frac{1 + \mu_p^2}{4} + \frac{4m_p^2}{Q_0^2} \approx 7.16, \quad (17)$$

$$b = 1 - \frac{4m_p^2}{Q_0^2} \approx -3.96, \quad (18)$$

$$c = \frac{\mu_p^2 - 1}{b^4} \approx 0.028. \quad (19)$$

In order to perform these calculations in an efficient way, we used a numerical method. The numerical integration is performed using the CalcHEP packages [59].

The present LHeC and the FCC-he are planned to generate e^-p collisions at energies from 1.30 TeV to 10 TeV [21, 44]. The LHeC is a suggested deep inelastic electron-nucleon scattering machine which has been planned to collide electrons with an energy from 60 GeV to possibly 140 GeV, with protons with an energy of 7 TeV. In addition, FCC-he is designed electrons with an energy from 250 GeV to 500 GeV, with protons with an energy of 50 TeV. The LHeC and the FCC-he physics programs will enable fundamentally new insights beyond the capabilities of the LHC for the anomalous coupling $W^+W^-\gamma$. In addition, the flexibility and large accessible energy range provides a wide range of possibilities to measure the new physics using very different approaches.

The high-luminosity and the low backgrounds of QCD give access to the process $e^-p \rightarrow e^-\gamma^*p \rightarrow \nu_e W^- p$ at all energies. Furthermore, the clean experimental environment and the good knowledge of the initial state allow precise measurements of the cross-section of the $\nu_e W^-$ signal, as well as of $\Delta\kappa_\gamma$ and λ_γ , respectively.

Fig. 3 shows the total cross-sections of the process $e^-p \rightarrow e^-\gamma^*p \rightarrow \nu_e W^- p$ as a function of $\Delta\kappa_\gamma$ for center-of-mass energies of $\sqrt{s} = 1.30, 1.98, 7.07, 10$ TeV at the LHeC and the FCC-he. The mechanism $e^-p \rightarrow e^-\gamma^*p \rightarrow \nu_e W^- p$ is dominant at $\sqrt{s} = 10$ TeV reaching a cross-section of 20 pb. A similar study on the cross-sections of the process $e^-p \rightarrow e^-\gamma^*p \rightarrow \nu_e W^- p$ as a function of λ_γ is presented in Fig. 4. In this case, the cross-section obtained is of 5 pb

at center-of-mass energy of $\sqrt{s} = 10$ TeV. In general, this process can be identified at all the energy stages of the LHeC and the FCC-he.

From Fig. 3 (and similarly in Fig. 7), in the case of 1.30 and 1.98 TeV where the center-of-mass energies are relatively low, there is an asymmetry of the cross-section values relative to the negative and positive values of the anomalous couplings $\Delta\kappa_\gamma$ and λ_γ . This is due to the cross terms of the anomalous couplings with SM terms. It is observed that this asymmetry decreased significantly due to the reduction of the effect of the SM in increasing center-of-mass energies.

B. Limits on the anomalous couplings $\Delta\kappa_\gamma$ and λ_γ at the LHeC and the FCC-he

One of the main purposes of this paper is to determine the best measurements of the anomalous couplings $\Delta\kappa_\gamma$ and λ_γ at the LHeC and the FCC-he. To carry out this purpose, we adopted a χ^2 analysis. The χ^2 function for our fit is defined as similar [61–64]:

$$\chi^2(\Delta\kappa_\gamma, \lambda_\gamma) = \left(\frac{\sigma_{SM} - \sigma_{BSM}(\sqrt{s}, \Delta\kappa_\gamma, \lambda_\gamma)}{\sigma_{SM} \sqrt{(\delta_{st})^2 + (\delta_{sys})^2}} \right)^2, \quad (20)$$

where $\sigma_{BSM}(\sqrt{s}, \Delta\kappa_\gamma, \lambda_\gamma)$ and σ_{SM} are the cross-section in the presence of beyond SM interactions and in the SM, respectively. $\delta_{st} = \frac{1}{\sqrt{N_{SM}}}$ is the statistical error and δ_{sys} is the systematic error. The number of events is given by $N_{SM} = \mathcal{L}_{int} \times \sigma_{SM} \times BR(W^\pm \rightarrow qq', l\nu_l)$, where \mathcal{L}_{int} is the integrated luminosity and $l = e^-, \mu$. For single W^- production at the LHeC and the FCC-he we classify their decay products according to the decomposition of W^- . In this paper, we consider that the W^- boson decay leptonically or hadronically for the signal. Thus, we assume that the branching ratios for W^- decays are: $BR(W^- \rightarrow qq') = 0.674$ for hadronic decays and $BR(W^- \rightarrow l\nu) = 0.213$ for light leptonic decays.

We examine in Figs. 5 and 6 the impact of center-of-mass energies $\sqrt{s} = 1.30, 1.98, 7.07, 10$ TeV and the luminosities $\mathcal{L} = 10, 50, 100, 500, 1000 \text{ fb}^{-1}$ on the anomalous couplings $\Delta\kappa_\gamma$ and λ_γ . The expected measurement for both $\Delta\kappa_\gamma$ and λ_γ is 10^{-2} for 7.07, 10 TeV and 100, 500, 1000 fb^{-1} , respectively. For other energy stages of the LHeC, the expected measurements on $\Delta\kappa_\gamma$ and λ_γ are an order of magnitude weaker. However, for all the energy and luminosity stages of the LHeC and the FCC-he the measurements on $\Delta\kappa_\gamma$ and λ_γ are accessible.

Estimations of the one-parameter limits on the anomalous couplings $\Delta\kappa_\gamma$ and λ_γ given in Eqs. (8) and (9) are presented in Table I, where one of the anomalous couplings is fixed to zero. In Table I, we consider the leptonic and hadronic decay channels of the process $e^-p \rightarrow e^- \gamma^* p \rightarrow \nu_e W^- p$ at the LHeC with $\sqrt{s} = 1.30, 1.98$ TeV and integrated luminosities $\mathcal{L} = 10, 30, 50, 70, 100 \text{ fb}^{-1}$. A similar estimation for the anomalous couplings $\Delta\kappa_\gamma$ and λ_γ is presented in Table II, where in this case $\sqrt{s} = 7.07, 10$ TeV at the FCC-he with integrated luminosities $\mathcal{L} = 100, 300, 500, 700, 1000 \text{ fb}^{-1}$, respectively. From these tables, it is clear that in the leptonic channel the limits on the $\Delta\kappa_\gamma$ and λ_γ are of the order of magnitude of few times 10^{-3} to 10^{-2} . However, due to the larger branching ratio, the hadronic channel can improve the constraints by a factor of two or three with respect to the leptonic channel.

From Table II, our best limits for the anomalous couplings $\Delta\kappa_\gamma$ and λ_γ at the FCC-he are the following.

i) Limits on $\Delta\kappa_\gamma$ and λ_γ for $\sqrt{s} = 7.07 \text{ TeV}$, $\mathcal{L} = 1000 \text{ fb}^{-1}$ and $P_{e^-} = 0\%$:

$$\Delta\kappa_\gamma = \begin{array}{ll} |0.0033|, & 95\% \text{ C.L., leptonic,} \\ |0.0019|, & 95\% \text{ C.L., hadronic,} \end{array} \quad (21)$$

$$\lambda_\gamma = \begin{array}{ll} |0.0098|, & 95\% \text{ C.L., leptonic,} \\ |0.0073|, & 95\% \text{ C.L., hadronic.} \end{array} \quad (22)$$

ii) Limits on $\Delta\kappa_\gamma$ and λ_γ for $\sqrt{s} = 10 \text{ TeV}$, $\mathcal{L} = 1000 \text{ fb}^{-1}$ and $P_{e^-} = 0\%$:

$$\Delta\kappa_\gamma = \begin{array}{ll} |0.0031|, & 95\% \text{ C.L., leptonic,} \\ |0.0017|, & 95\% \text{ C.L., hadronic,} \end{array} \quad (23)$$

$$\lambda_\gamma = \begin{array}{ll} |0.0071|, & 95\% \text{ C.L., leptonic,} \\ |0.0053|, & 95\% \text{ C.L., hadronic.} \end{array} \quad (24)$$

The limits given in Eqs. (21)-(24) are consistent with the corresponding ones of Table I of Ref. [10] for the anomalous couplings $\Delta\kappa_\gamma$ and λ_γ .

C. Impact of the polarized electron beam on the cross-section of the process $e^-p \rightarrow e^-\gamma^*p \rightarrow \nu_e W^-p$ at the LHeC and the FCC-he

In the previous sub-sections, the results for the cross-section of the process $e^-p \rightarrow e^-\gamma^*p \rightarrow \nu_e W^-p$, as well as of the anomalous parameters $\Delta\kappa_\gamma$ and λ_γ are presented with unpolarized electron beam. In this sub-section we discuss the impact of the polarized electron beam in the cross-section and in the anomalous parameters of the aforementioned process.

It is worth noting that a polarized electron beam provides a method to investigate the SM and to diagnose new physics beyond the SM. Proper selection of the electron beam polarization may, therefore be used to enhance the new physics signal and also to considerably suppress backgrounds. We select beam polarization as $P_{e^-} = -80\%$ to enhance our physical process. In addition, as we already mentioned in subsection A, the chiral nature of the weak coupling to fermions results in significant possible enhancements in $\nu_e W^-$ production, as indicated in Figs. 7 and 8.

Our results for joint variation of the cross-section with the $\Delta\kappa_\gamma$ or λ_γ couplings are shown in Figs. 7 and 8. In each case, we consider the four center-of-mass energies stages of the FCC-he with their respective integrated luminosities.

The $\sigma(e^-p \rightarrow e^-\gamma^*p \rightarrow \nu_e W^-p)$ curves as a function of each of the anomalous couplings, setting the other to its SM value of zero, is shown in Figs. 7 and 8. In this case we consider polarized electron beam with $P_{e^-} = -80\%$. The following results for the cross-section of the process $\sigma(e^-p \rightarrow e^-\gamma^*p \rightarrow \nu_e W^-p)$ are obtained: $\sigma(\sqrt{s}, \Delta\kappa_\gamma) = 30 \text{ pb}$ for $-3 \leq \Delta\kappa_\gamma \leq 3$ and $\sigma(\sqrt{s}, \lambda_\gamma) = 10 \text{ pb}$ for $-2 \leq \lambda_\gamma \leq 2$, in both cases with $\sqrt{s} = 10 \text{ TeV}$. From these figures a difference of a factor of 4-10 for the minimum and maximum center-of-mass energies of $1.30 - 10 \text{ TeV}$ is obtained.

D. Impact of the polarized electron beam on the limits of the anomalous couplings $\Delta\kappa_\gamma$ and λ_γ at the LHeC and the FCC-he

In this sub-section, we presented a model-independent global fit on the anomalous couplings $\Delta\kappa_\gamma$ and λ_γ . To carry out this, we made use of the total cross-section for the process $e^-p \rightarrow e^-\gamma^*p \rightarrow \nu_e W^-p$ in e^-p collisions. The results of the fit for the four FCC-he energy stages with their respective luminosities are shown in Figs. 9 and 10.

Figs. 9 and 10 show the summary plot illustrating the limits that can be obtained of the process $e^-p \rightarrow e^-\gamma^*p \rightarrow \nu_e W^- p$ on the couplings $\Delta\kappa_\gamma$ and λ_γ . We consider the following center-of-mass energies, luminosities and polarization of the electron beam $\sqrt{s} = 1.30, 1.98, 1.07, 10 \text{ TeV}$, $\mathcal{L} = 10, 50, 100, 500, 1000 \text{ fb}^{-1}$ and $P_{e^-} = -80\%$, respectively. For comparison, on the same panel we give the constraints from CMS (grey) Collaborations at the LHC.

To complement our study on the anomalous parameters $\Delta\kappa_\gamma$ and λ_γ through the process $e^-p \rightarrow e^-\gamma^*p \rightarrow \nu_e W^- p$ with polarized electron beam and considering the parameters of the LHeC and the FCC-he, we give limits for the anomalous couplings of the W^- -boson in Tables III and IV. These limits show the best measurement is compared with the unpolarized case illustrated in Tables I and II.

The following limits are set on the couplings $\Delta\kappa_\gamma$ and λ_γ at the FCC-he and with polarized electron beam when one parameter is allowed to vary and the others are set to their SM values of zero.

i) Limits on $\Delta\kappa_\gamma$ and λ_γ for $\sqrt{s} = 7.07 \text{ TeV}$, $\mathcal{L} = 1000 \text{ fb}^{-1}$ and $P_{e^-} = -80\%$:

$$\Delta\kappa_\gamma = \begin{array}{ll} |0.0025|, & 95\% \text{ C.L., leptonic,} \\ |0.0014|, & 95\% \text{ C.L., hadronic,} \end{array} \quad (25)$$

$$\lambda_\gamma = \begin{array}{ll} |0.0085|, & 95\% \text{ C.L., leptonic,} \\ |0.0063|, & 95\% \text{ C.L., hadronic.} \end{array} \quad (26)$$

ii) Limits on $\Delta\kappa_\gamma$ and λ_γ for $\sqrt{s} = 10 \text{ TeV}$, $\mathcal{L} = 1000 \text{ fb}^{-1}$ and $P_{e^-} = -80\%$:

$$\Delta\kappa_\gamma = \begin{array}{ll} |0.0023|, & 95\% \text{ C.L., leptonic,} \\ |0.0013|, & 95\% \text{ C.L., hadronic,} \end{array} \quad (27)$$

$$\lambda_\gamma = \begin{array}{ll} |0.0061|, & 95\% \text{ C.L., leptonic,} \\ |0.0046|, & 95\% \text{ C.L., hadronic.} \end{array} \quad (28)$$

A direct comparison of the results shown in the Eqs. (21)-(24) for the unpolarized case and Eqs. (25)-(28) for the case with polarized electron beam for the anomalous couplings $\Delta\kappa_\gamma$ and λ_γ clearly shows that the polarized electron beam effect translates into a factor of 1.35 in the measurement of $\Delta\kappa_\gamma$ and λ_γ .

On the other hand, it is appropriate to mention that the limits shown in Tables I-IV are competitive with the experimental and phenomenological limits obtained by the ATLAS,

CMS, CDF, D0, ALEP, DELPHI, L3 and OPAL Collaborations, as well as by the ILC and the CEPC which are shown in Table I of Ref. [10].

IV. CONCLUSIONS

The production cross-section of the process $e^-p \rightarrow e^-\gamma^*p \rightarrow \nu_e W^-p$ in the SM is 1.50 pb in the case of unpolarized electron beam and of 3 pb for the case of polarized electron beam with $\sqrt{s} = 10$ TeV as is shown in Figs. 3, 4 and 7, 8. In addition, one can see the $\sigma(e^-p \rightarrow e^-\gamma^*p \rightarrow \nu_e W^-p)$ increases monotonically with $\Delta\kappa_\gamma$ and the absolute value of λ_γ within the parameter region allowed by current experiments, this is enough to probe anomalous triple gauge couplings contributions. These couplings could reach $\mathcal{O}(10^{-3})$ when $\mathcal{L} = 1000 \text{ fb}^{-1}$.

From the results in Tables I-IV and Figs. 3-10, we could see a significant improvement in the measurement for $\Delta\kappa_\gamma$ and λ_γ compared to the present ATLAS, CMS, CDF, D0, ALEP, DELPHI, L3 and OPAL collaborations bounds (see Table I of Ref. [10]).

We have presented new searches of anomalous $W^+W^-\gamma$ trilinear gauge boson couplings from $e^-p \rightarrow e^-\gamma^*p \rightarrow \nu_e W^-p$ channel analyzing $(10 - 1000) \text{ fb}^{-1}$ of integrated luminosities and center-of-mass energies $\sqrt{s} = 1.30, 1.98, 7.07, 10$ TeV, respectively. We set model-independent limits on anomalous triple gauge couplings $\Delta\kappa_\gamma$ and λ_γ for the final states $\nu_e W^-$ at the 95% C.L.: $\Delta\kappa_\gamma = \pm 0.0017$, $\lambda_\gamma = \pm 0.0053$ (unpolarized electron beam) and $\Delta\kappa_\gamma = \pm 0.0013$, $\lambda_\gamma = \pm 0.0046$ (polarized electron beam) with $\sqrt{s} = 10$ TeV and $\mathcal{L} = 1000 \text{ fb}^{-1}$ for both cases. The W^- -boson is identified through the hadronic decays channel. In addition, it is worth mentioning that the impact of the polarized electron beam translates into a factor of 1.35 with respect to the non-polarized case (see Tables I-IV).

In conclusion, the measurement of the $e^-p \rightarrow e^-\gamma^*p \rightarrow \nu_e W^-p$ channel at the LHeC and the FCC-he would provide a promising opportunity to probe the anomalous couplings $\Delta\kappa_\gamma$ and λ_γ without the complications of other couplings especially QCD backgrounds, and therefore improve our knowledge of the gauge sector. Furthermore, for future measurement of $\Delta\kappa_\gamma$ and λ_γ , we expect complementarily studies with different electron beam polarizations, as well as a more realistic detector-level analysis will be very useful.

TABLE I: Estimations of the 95% C.L. prospects for the anomalous couplings $\Delta\kappa_\gamma$ and λ_γ in the leptonic and hadronic decay channels of the process $e^-p \rightarrow e^-\gamma^*p \rightarrow \nu_e W^- p$ at the LHeC with $\sqrt{s} = 1.30, 1.98$ TeV and integrated luminosities of $\mathcal{L} = 10, 30, 50, 70, 100 \text{ fb}^{-1}$. All the limits for $\Delta\kappa_\gamma(\lambda_\gamma)$ are obtained while the other coupling is fixed to their SM value of zero.

95% C.L.		$\sqrt{s} = 1.30 \text{ TeV}$		$\sqrt{s} = 1.98 \text{ TeV}$	
	$\mathcal{L} \text{ (} fb^{-1} \text{)}$	Channel			
		Leptonic	Hadronic	Leptonic	Hadronic
$\Delta\kappa_\gamma$	10	[-0.0607, 0.0571]	[-0.0336, 0.0325]	[-0.0499, 0.0473]	[-0.0277, 0.0269]
	30	[-0.0345, 0.0333]	[-0.0192, 0.0189]	[-0.0285, 0.0276]	[-0.0159, 0.0156]
	50	[-0.0266, 0.0259]	[-0.0149, 0.0146]	[-0.0220, 0.0214]	[-0.0123, 0.0121]
	70	[-0.0224, 0.0219]	[-0.0125, 0.0124]	[-0.0185, 0.0181]	[-0.0103, 0.0102]
	100	[-0.0187, 0.0184]	[-0.0105, 0.0104]	[-0.0155, 0.0152]	[-0.0086, 0.0086]
λ_γ	10	[-0.1546, 0.1546]	[-0.1159, 0.1159]	[-0.1022, 0.1022]	[-0.0766, 0.0766]
	30	[-0.1175, 0.1175]	[-0.0881, 0.0881]	[-0.0777, 0.0777]	[-0.0582, 0.0582]
	50	[-0.1034, 0.1034]	[-0.0775, 0.0775]	[-0.0684, 0.0684]	[-0.0512, 0.0512]
	70	[-0.0950, 0.0950]	[-0.0712, 0.0712]	[-0.0628, 0.0628]	[-0.0471, 0.0471]
	100	[-0.0869, 0.0869]	[-0.0652, 0.0652]	[-0.0575, 0.0575]	[-0.0431, 0.0431]

Acknowledgments

A. G. R. and M. A. H. R. thank SNI and PROFOCIE (México).

[1] S. L. Glashow, *Nucl. Phys.* **22**, 579 (1961).

[2] A. Salam, J. C., *Phys. Lett.* **13**, 168 (1964).

TABLE II: Estimations of the 95% C.L. prospects for the anomalous couplings $\Delta\kappa_\gamma$ and λ_γ in the leptonic and hadronic decay channels of the process $e^-p \rightarrow e^-\gamma^*p \rightarrow \nu_e W^- p$ at the FCC-he with $\sqrt{s} = 7.07, 10$ TeV and integrated luminosities of $\mathcal{L} = 100, 300, 500, 700, 1000 \text{ fb}^{-1}$. All the limits for $\Delta\kappa_\gamma(\lambda_\gamma)$ are obtained while the other coupling is fixed to their SM value of zero.

95% C.L.		$\sqrt{s} = 7.07 \text{ TeV}$		$\sqrt{s} = 10 \text{ TeV}$	
	$\mathcal{L} \text{ (} fb^{-1} \text{)}$	Channel			
		Leptonic	Hadronic	Leptonic	Hadronic
$\Delta\kappa_\gamma$	100	[-0.0107, 0.0106]	[-0.0059, 0.0059]	[-0.0100, 0.0099]	[-0.0055, 0.0055]
	300	[-0.0061, 0.0061]	[-0.0034, 0.0034]	[-0.0057, 0.0057]	[-0.0032, 0.0032]
	500	[-0.0047, 0.0047]	[-0.0026, 0.0026]	[-0.0044, 0.0044]	[-0.0025, 0.0025]
	700	[-0.0040, 0.0040]	[-0.0022, 0.0022]	[-0.0037, 0.0037]	[-0.0021, 0.0021]
	1000	[-0.0033, 0.0033]	[-0.0019, 0.0019]	[-0.0031, 0.0031]	[-0.0017, 0.0017]
λ_γ	100	[-0.0175, 0.0175]	[-0.0131, 0.0131]	[-0.0127, 0.0127]	[-0.0095, 0.0095]
	300	[-0.0133, 0.0133]	[-0.0099, 0.0099]	[-0.0096, 0.0096]	[-0.0072, 0.0072]
	500	[-0.0117, 0.0117]	[-0.0088, 0.0088]	[-0.0085, 0.0085]	[-0.0063, 0.0063]
	700	[-0.0107, 0.0107]	[-0.0080, 0.0080]	[-0.0078, 0.0078]	[-0.0058, 0.0058]
	1000	[-0.0098, 0.0098]	[-0.0073, 0.0073]	[-0.0071, 0.0071]	[-0.0053, 0.0053]

- [3] S. Weinberg, *Phys. Rev. Lett.* **19**, 1264 (1967).
- [4] Oliver Brüning, John Jowett, Max Klein, Dario Pellegrini, Daniel Schulte and Frank Zimmermann, EDMS 17979910 FCC-ACC-RPT-0012, V1.0, 6 April, 2017.
<https://fcc.web.cern.ch/Documents/FCCheBaselineParameters.pdf>.
- [5] J. L. A. Fernandez, *et al.*, [LHeC Study Group], *J. Phys.* **G39**, 075001 (2012).
- [6] J. L. A. Fernandez, *et al.*, [LHeC Study Group], arXiv:1211.5102.
- [7] J. L. A. Fernandez, *et al.*, arXiv:1211.4831.
- [8] Huan-Yu, Bi, Ren-You Zhang, Xing-Gang Wu, Wen-Gan Ma, Xiao-Zhou Li and Samuel Owusu, *Phys. Rev.* **D95**, 074020 (2017).
- [9] Y. C. Acar, A. N. Akay, S. Beser, H. Karadeniz, U. Kaya, B. B. Oner, S. Sultansoy, *Nuclear*

TABLE III: Estimations of the 95% C.L. prospects for the anomalous couplings $\Delta\kappa_\gamma$ and λ_γ in the leptonic and hadronic decay channels of the process $e^-p \rightarrow e^-\gamma^*p \rightarrow \nu_e W^- p$ at the LHeC with $\sqrt{s} = 1.30, 1.98$ TeV and integrated luminosities of $\mathcal{L} = 10, 30, 50, 70, 100 \text{ fb}^{-1}$. All the limits for $\Delta\kappa_\gamma(\lambda_\gamma)$ are obtained while the other coupling is fixed to their SM value of zero. We considered polarized electron beam with $P_e = -80\%$.

95% C.L.		$\sqrt{s} = 1.30 \text{ TeV}$		$\sqrt{s} = 1.98 \text{ TeV}$	
	$\mathcal{L} \text{ (} fb^{-1} \text{)}$	Channel			
		Leptonic	Hadronic	Leptonic	Hadronic
$\Delta\kappa_\gamma$	10	[-0.0449, 0.0429]	[-0.0249, 0.0243]	[-0.0369, 0.0355]	[-0.0205, 0.0201]
	30	[-0.0256, 0.0250]	[-0.0143, 0.0141]	[-0.0211, 0.0206]	[-0.0118, 0.0117]
	50	[-0.0198, 0.0194]	[-0.0110, 0.0109]	[-0.0163, 0.0160]	[-0.0091, 0.0090]
	70	[-0.0167, 0.0164]	[-0.0093, 0.0092]	[-0.0137, 0.0135]	[-0.0076, 0.0076]
	100	[-0.0139, 0.0138]	[-0.0078, 0.0077]	[-0.0113, 0.0113]	[-0.0064, 0.0064]
λ_γ	10	[-0.1335, 0.1335]	[-0.1001, 0.1001]	[-0.0882, 0.0882]	[-0.0661, 0.0661]
	30	[-0.1014, 0.1014]	[-0.0760, 0.0760]	[-0.0670, 0.0670]	[-0.0502, 0.0502]
	50	[-0.0892, 0.0892]	[-0.0669, 0.0669]	[-0.0590, 0.0590]	[-0.0442, 0.0442]
	70	[-0.0820, 0.0820]	[-0.0615, 0.0615]	[-0.0542, 0.0542]	[-0.0406, 0.0406]
	100	[-0.0750, 0.0750]	[-0.0562, 0.0562]	[-0.0496, 0.0496]	[-0.0372, 0.0372]

Inst. and Methods in Physics Research **A871**, 47 (2017).

- [10] A. A. Billur, M. Köksal, A. Gutiérrez-Rodríguez and M. A. Hernández-Ruiz, arXiv:1909.10299 [hep-ph]
- [11] U. Baur and D. Zeppenfeld, *Phys. Lett.* **B201**, 383 (1988).
- [12] K. Hagiwara, R. D. Peccei, D. Zeppenfeld and K. Hikasa, *Nucl. Phys.* **B282**, 253 (1987).
- [13] K. Hagiwara, S. Ishihara, R. Szalapski and D. Zeppenfeld, *Phys. Lett.* **B283**, 353 (1992).
- [14] M. Diehl and O. Nachtmann, *Z. Phys.* **C62**, 397 (1994).
- [15] I Sahin and A. A. Billur, *Phys. Rev.* **D83**, 035011 (2011).
- [16] I. T. Cakir, O. Cakir, A. Senol and A. T. Tasci, *Acta Physica Polonica* **B45**, 1947 (2014).

TABLE IV: Estimations of the 95% C.L. prospects for the anomalous couplings $\Delta\kappa_\gamma$ and λ_γ in the leptonic and hadronic decay channels of the process $e^-p \rightarrow e^-\gamma^*p \rightarrow \nu_e W^- p$ at the FCC-he with $\sqrt{s} = 7.07, 10$ TeV and integrated luminosities of $\mathcal{L} = 100, 300, 500, 700, 1000 \text{ fb}^{-1}$. All the limits for $\Delta\kappa_\gamma(\lambda_\gamma)$ are obtained while the other coupling is fixed to their SM value of zero. We considered polarized electron beam with $P_e = -80\%$.

95% C.L.		$\sqrt{s} = 7.07 \text{ TeV}$		$\sqrt{s} = 10 \text{ TeV}$	
	$\mathcal{L} \text{ (} fb^{-1} \text{)}$	Channel			
		Leptonic	Hadronic	Leptonic	Hadronic
$\Delta\kappa_\gamma$	100	[-0.0080, 0.0079]	[-0.0044, 0.0044]	[-0.0074, 0.0074]	[-0.0041, 0.0041]
	300	[-0.0045, 0.0045]	[-0.0025, 0.0025]	[-0.0042, 0.0042]	[-0.0024, 0.0024]
	500	[-0.0035, 0.0035]	[-0.0020, 0.0020]	[-0.0033, 0.0033]	[-0.0018, 0.0018]
	700	[-0.0030, 0.0030]	[-0.0016, 0.0016]	[-0.0028, 0.0028]	[-0.0015, 0.0015]
	1000	[-0.0025, 0.0025]	[-0.0014, 0.0014]	[-0.0023, 0.0023]	[-0.0013, 0.0013]
λ_γ	100	[-0.0151, 0.0151]	[-0.0113, 0.0113]	[-0.0110, 0.0110]	[-0.0082, 0.0082]
	300	[-0.0115, 0.0115]	[-0.0086, 0.0086]	[-0.0083, 0.0083]	[-0.0062, 0.0062]
	500	[-0.0101, 0.0101]	[-0.0075, 0.0075]	[-0.0073, 0.0073]	[-0.0055, 0.0055]
	700	[-0.0093, 0.0093]	[-0.0069, 0.0069]	[-0.0067, 0.0067]	[-0.0050, 0.0050]
	1000	[-0.0085, 0.0085]	[-0.0063, 0.0063]	[-0.0061, 0.0061]	[-0.0046, 0.0046]

- [17] Seyed Mohsen Etesami, *et al.*, *Eur. Phys. J.* **C76**, 533 (2016).
- [18] V. Ari, A. A. Billur, S. C. Inan and M. Köksal, *Nucl. Phys.* **B906**, 211 (2016).
- [19] S. Atag and I. T. Cakir, *Phys. Rev.* **D63**, 033004 (2001).
- [20] S. Atag and I. Sahin, *Phys. Rev.* **D64**, 095002 (2001).
- [21] B. Sahin, *Phys. Scripta* **79**, 065101 (2009).
- [22] J. Papavassiliou and K. Philippides, *Phys. Rev.* **D60**, 113007 (1999).
- [23] D. Choudhury, J. Kalinowski and A. Kulesza, *Phys. Lett.* **B457**, 193 (1999).
- [24] E. Chapon, C. Royon and O. Kepka, *Phys. Rev.* **D81**, 074003 (2010).
- [25] John Ellis, Shao-Feng Ge, Hong-Jian He, Rui-Qing Xiao, arXiv:1902.06631 [hep-ph].

- [26] K. J. F. Gaemers and G. J. Gounaris, *Z. Phys.* **C1**, 259 (1979).
- [27] A. De Rujula, M. B. Gavela, P. Hernandez and E. Masso, *Nucl. Phys.* **B384**, 3 (1992).
- [28] K. Hagiwara, S. Ishihara, R. Szalapski and D. Zeppenfeld, *Phys. Rev.* **D48**, 2182 (1993).
- [29] I. F. Ginzburg, arXiv:1508.06581 [hep-ph].
- [30] I. F. Ginzburg, G. L. Kotkin, S. L. Panfil, V. G. Serbo and V. I. Telnov, *Nucl. Instrum. Meth.* **A219**, 5 (1984).
- [31] S. J. Brodsky, T. Kinoshita and H. Terazawa, *Phys. Rev.* **D4**, 1532 (1971).
- [32] V. M. Budnev, I. F. Ginzburg, G. V. Meledin and V. G. Serbo, *Phys. Rep.* **15**, 181 (1975).
- [33] H. Terazawa, *Rev. Mod. Phys.* **45**, 615 (1973).
- [34] J. M. Yang, *Annals Phys.* **316**, 529 (2005).
- [35] G. Baur, *et al.*, *Phys. Rep.* **364**, 359 (2002).
- [36] K. Piotrkowski, *Phys. Rev.* **D63**, 071502 (2001).
- [37] A. Abulencia, *et al.*, [CDF Collaboration], *Phys. Rev. Lett.* **98**, 112001 (2007).
- [38] T. Aaltonen, *et al.*, [CDF Collaboration], *Phys. Rev. Lett.* **102**, 222002 (2009).
- [39] T. Aaltonen, *et al.*, [CDF Collaboration], *Phys. Rev. Lett.* **102**, 242001 (2009).
- [40] S. Chatrchyan, *et al.*, [CMS Collaboration], *JHEP* **1201**, 052 (2012).
- [41] S. Chatrchyan, *et al.*, [CMS Collaboration], *JHEP* **1211**, 080 (2012).
- [42] V. M. Abazov, *et al.*, [D0 Collaboration], *Phys. Rev.* **D88**, 012005 (2013).
- [43] S. Chatrchyan, *et al.*, [CMS Collaboration], *JHEP* **07**, 116 (2013).
- [44] S. C. Inan, *Phys. Rev.* **D81**, 115002 (2010).
- [45] S. C. Inan, *Nucl. Phys.* **B897**, 289 (2015).
- [46] S. C. Inan, *Int. J. Mod. Phys.* **A26**, 3605 (2011).
- [47] I. Sahin and S. C. Inan, *JHEP* **0909**, 069 (2009).
- [48] S. Atag, S. C. Inan and I. Sahin, *JHEP* **1009**, 042 (2010).
- [49] I. Sahin and B. Sahin, *Phys. Rev.* **D86**, 115001 (2012).
- [50] B. Sahin and A. A. Billur, *Phys. Rev.* **D86**, 074026 (2012).
- [51] A. Senol, *Int. J. Mod. Phys.* **A29**, 1450148 (2014).
- [52] A. Senol, *Phys. Rev.* **D87**, 073003 (2013).
- [53] S. Fichet, G. von Gersdorff, B. Lenzi, C. Royon and M. Saimpert, *JHEP* **1502**, 165 (2015).
- [54] H. Sun, *Phys. Rev.* **D90**, 035018 (2014).
- [55] H. Sun, *Nucl. Phys.* **B886**, 691 (2014).

- [56] H. Sun, Y. J. Zhou and H. S. Hou, *JHEP* **1502**, 064 (2015).
- [57] A. Senol and M. Köksal, *JHEP* **1503**, 139 (2015).
- [58] XiaoJuan Wang, Hao Sun and Xuan Luo, *Adv. High Energy Phys.* **2017**, 4693213 (2017).
- [59] A. Belyaev, N. D. Christensen and A. Pukhov, *Comput. Phys. Commun.* **184**, 1729 (2013).
- [60] O. Bruening and M. Klein, *Mod. Phys. Lett. A28*, 1330011 (2013).
- [61] M. A. Hernández-Ruíz, A. Gutiérrez-Rodríguez, M. Köksal and A. A. Billur, *Nucl. Phys.* **B941**, 646 (2019).
- [62] M. Köksal, A. A. Billur, A. Gutiérrez-Rodríguez and M. A. Hernández-Ruíz, *Int. J. Mod. Phys.* **A34**, 1950076 (2019).
- [63] A. Gutiérrez-Rodríguez, M. A. Hernández-Ruíz, M. Köksal and A. A. Billur, arXiv:1903.04135 [hep-ph].
- [64] M. Köksal, A. A. Billur, A. Gutiérrez-Rodríguez and M. A. Hernández-Ruíz, arXiv:1905.02564 [hep-ph].

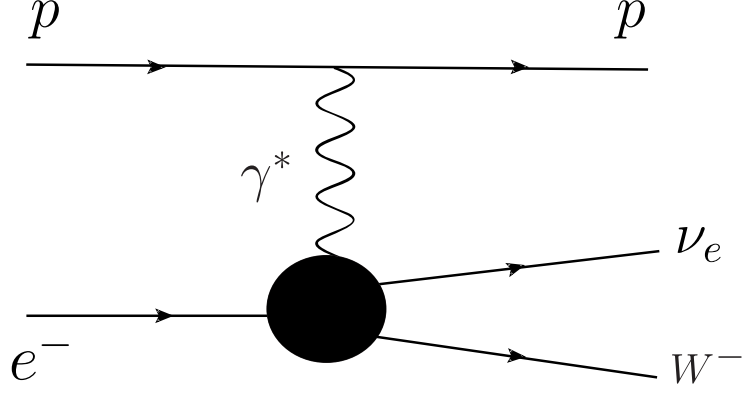


FIG. 1: A schematic diagram for the process $e^- p \rightarrow e^- \gamma^* p \rightarrow \nu_e W^- p$.

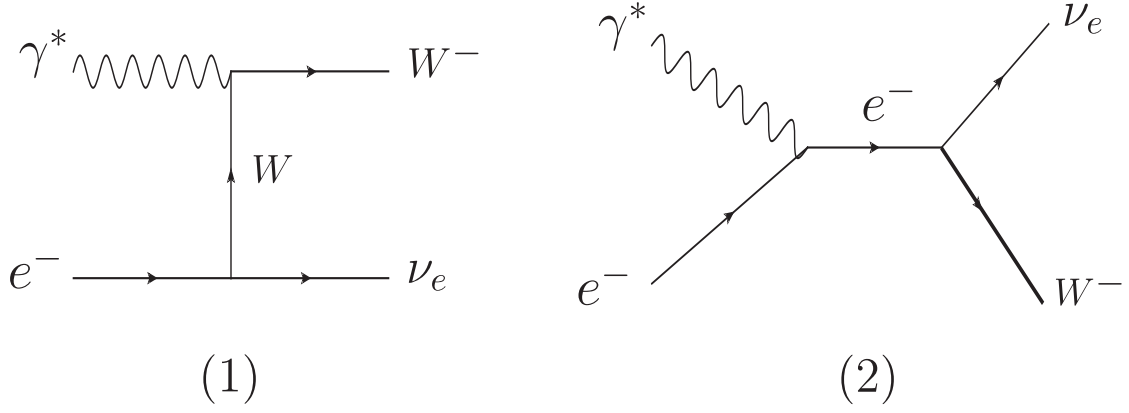


FIG. 2: Feynman diagrams contributing to the subprocess $\gamma^* e^- \rightarrow \nu_e W^-$.

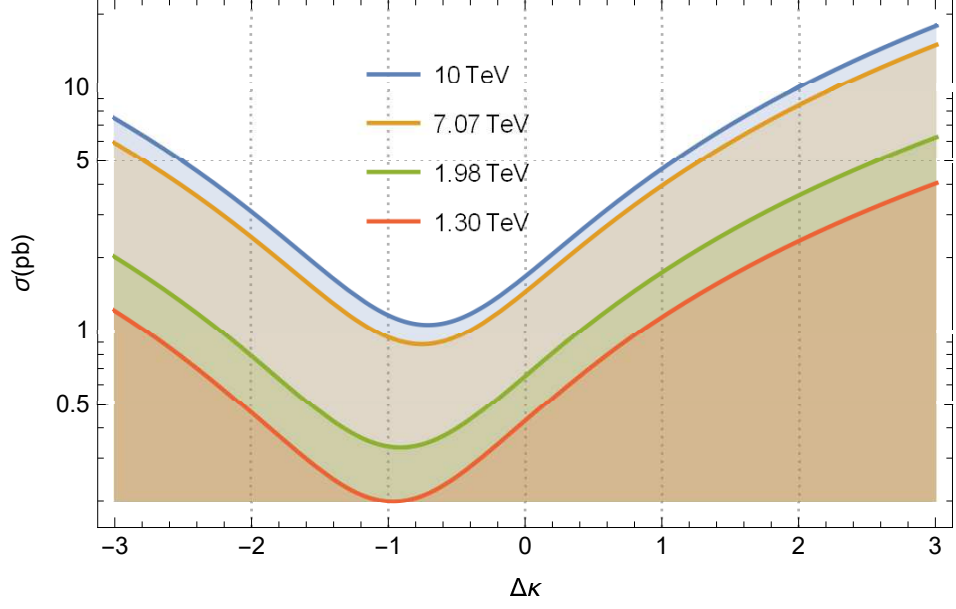


FIG. 3: The total cross sections of the process $e^-p \rightarrow e^-\gamma^*p \rightarrow \nu_e W^-p$ as a function of $\Delta\kappa_\gamma$ for center-of-mass energies of $\sqrt{s} = 1.30, 1.98, 7.07, 10$ TeV at the LHeC and the FCC-he.

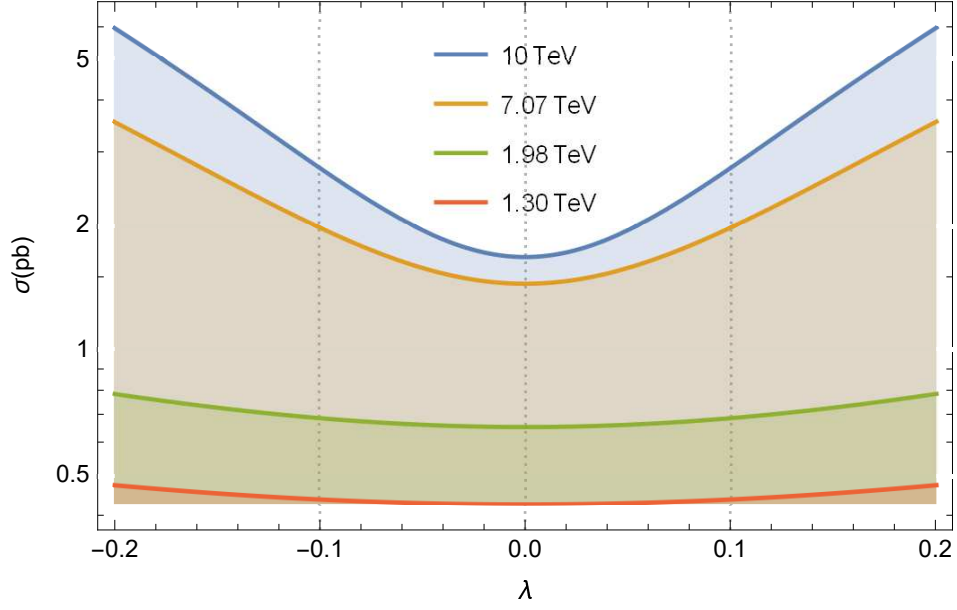


FIG. 4: Same as in Fig. 3, but for λ_γ .

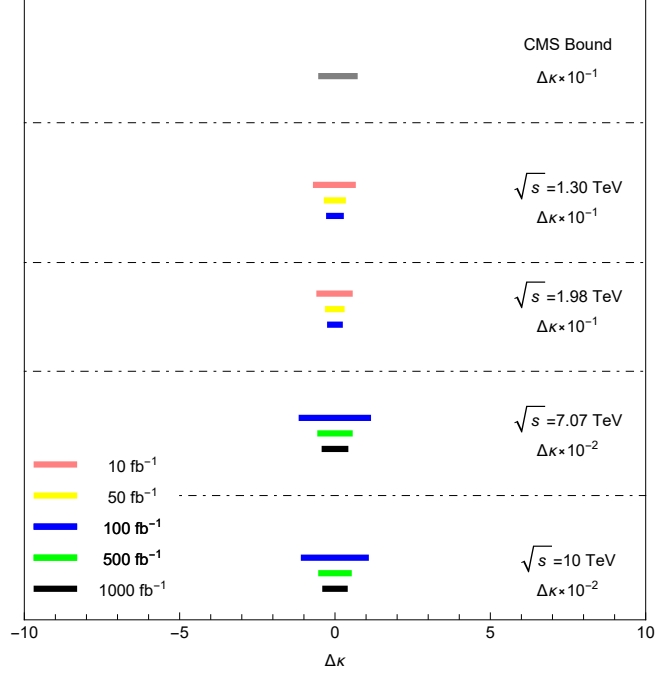


FIG. 5: Comparison of precisions at the LHeC and the FCC-he to the anomalous coupling $\Delta\kappa_\gamma$ for center-of-mass energies $\sqrt{s} = 1.30, 1.98, 1.07, 10$ TeV and luminosities $\mathcal{L} = 10, 50, 100, 500, 1000$ fb $^{-1}$. We consider the process $e^-p \rightarrow e^-\gamma^*p \rightarrow \nu_e W^- p$. We include the CMS bound.

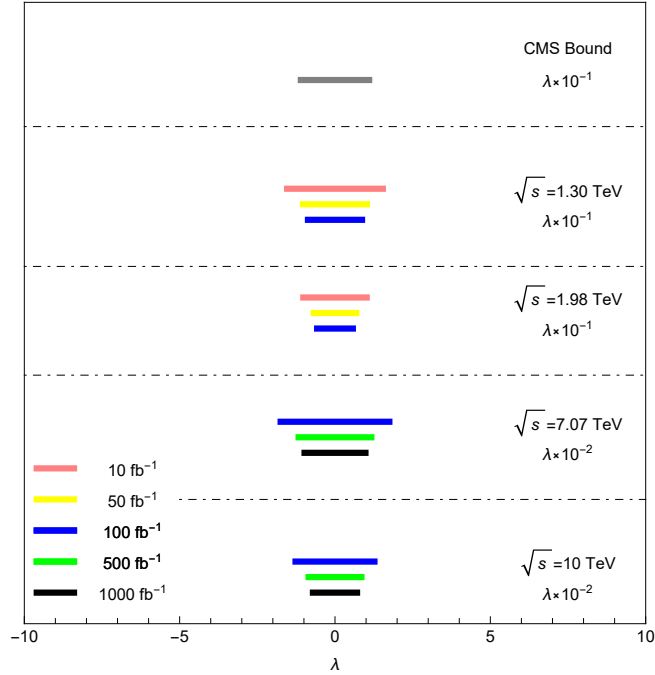


FIG. 6: Same as in Fig. 5, but for λ_γ .

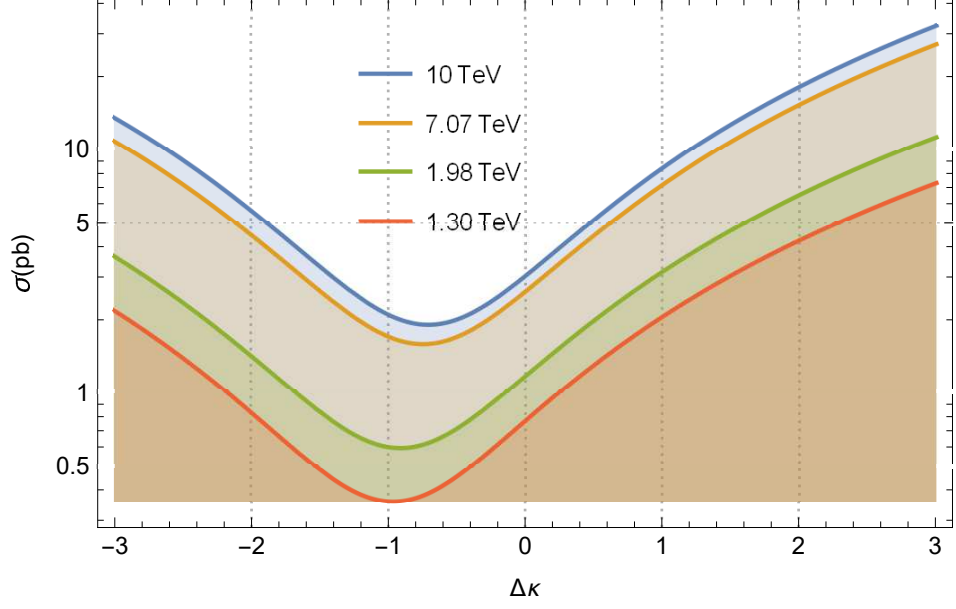


FIG. 7: Same as in Fig. 3, but with polarized electron beam.

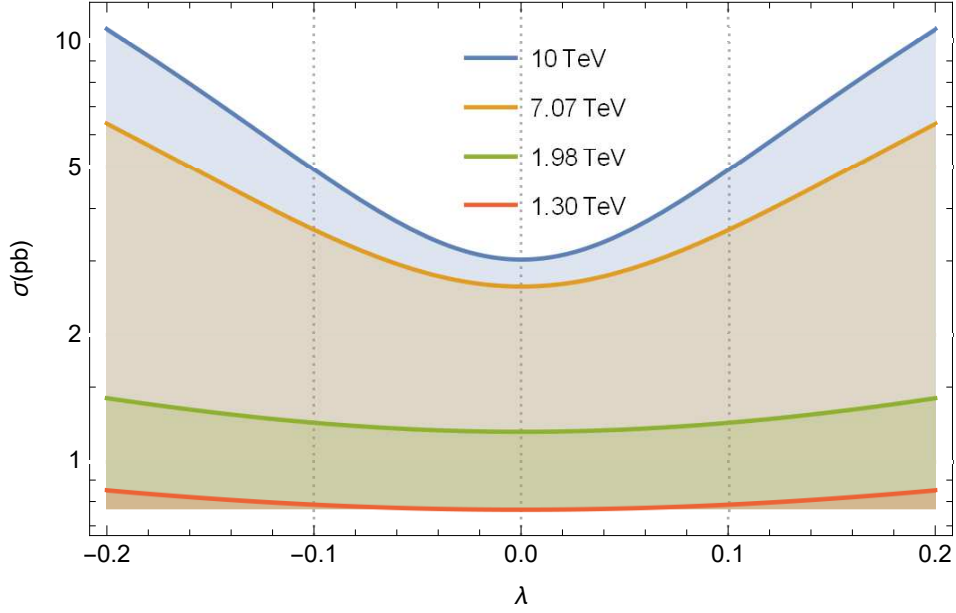


FIG. 8: Same as in Fig. 4, but with polarized electron beam.

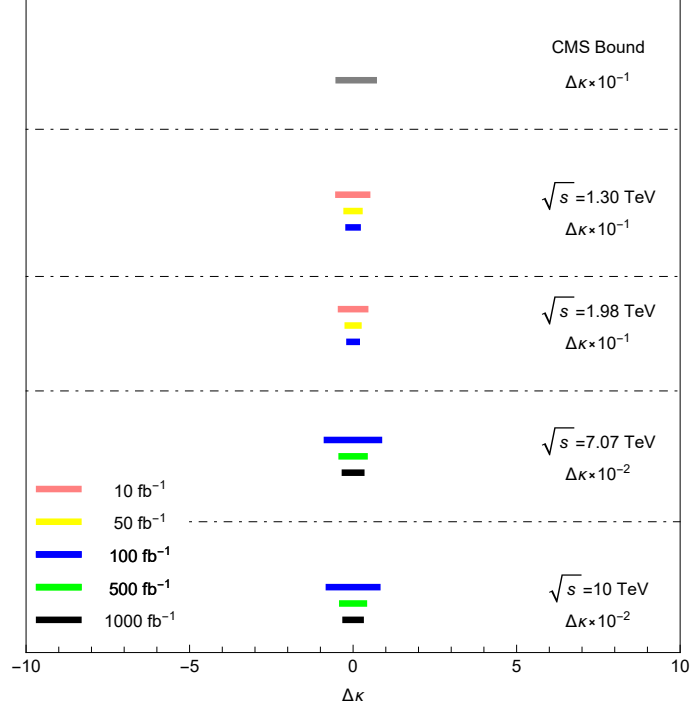


FIG. 9: Same as in Fig. 5, but with polarized electron beam.

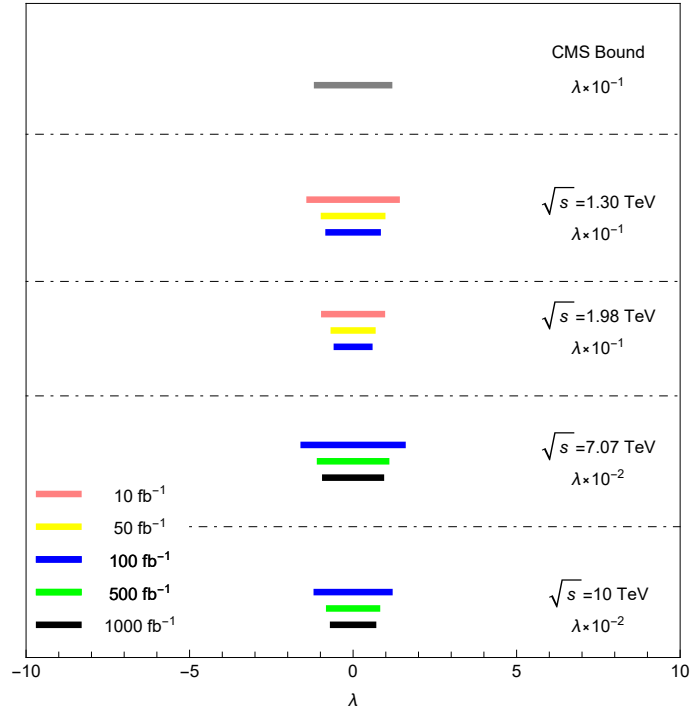


FIG. 10: Same as in Fig. 6, but with polarized electron beam.